Water clarity response to climate warming and wetting of the Inner Mongolia-Xinjiang Plateau: A remote sensing approach

Running head: Water clarity response to climate change

List of authors:

Yibo Zhang[1, 2]

Email: ybzhang@niglas.ac.cn

Kun Shi[1, 2, 3]

Email: kshi@niglas.ac.cn

Yunlin Zhang[1*, 2]

Email: ylzhang@niglas.ac.cn

Max Jacobo Moreno-Madriñán[4]

Email: mmorenom@iu.edu

Xuan Xu[1]

Email: xxu@niglas.ac.cn

Yongqiang Zhou[1, 2]

Email: yqzhou@niglas.ac.cn

Boqiang Qin[1, 2]

Email: qinbq@niglas.ac.cn

Guangwei Zhu[1, 2]

Email: gwzhu@niglas.ac.cn

Erik Jeppesen[5, 6, 7, 8]

Email: ej@bios.au.dk

This is the author's manuscript of the article published in final edited form as:

Zhang, Y., Shi, K., Zhang, Y., Moreno-Madriñán, M. J., Xu, X., Zhou, Y., Qin, B., Zhu, G., & Jeppesen, E. (2021). Water clarity response to climate warming and wetting of the Inner Mongolia-Xinjiang Plateau: A remote sensing approach. Science of The Total Environment, 796, 148916. https://doi.org/10.1016/j.scitotenv.2021.148916

Institutional affiliations

[1] State Key Laboratory of Lake Science and Environment, Nanjing Institute of Geography and Limnology, Chinese Academy of Sciences, Nanjing 210008, China

[2] University of the Chinese Academy of Sciences, Beijing 100049, China

[3] CAS Center for Excellence in Tibetan Plateau Earth Sciences, Chinese Academy of Sciences, Beijing 100101, China

[4] Department of Environmental Health, Indiana University Richard M Fairbanks School of Public Health, Indianapolis, IN 46202, USA

[5] Department of Bioscience and Arctic Research Centre, Aarhus University, Vejlsøvej 25, DK-8600 Silkeborg, Denmark

[6] Sino−Danish Centre for Education and Research, Beijing 100190, China

[7] Limnology Laboratory, Department of Biological Sciences and Centre for Ecosystem Research and Implementation, Middle East Technical University, Ankara, Turkey

[8] Institute of Marine Sciences, Middle East Technical University, Mersin, Turkey

[*]Corresponding author: Yunlin Zhang, Nanjing Institute of Geography and Limnology, Chinese Academy of Sciences, 73 East Beijing Road, Nanjing 210008, P. R. China, Tel: +86-25-86882198, Fax: +86-25-57714759, E-mail: ylzhang@niglas.ac.cn.

Abstract: Water clarity (generally quantified as the Secchi disk depth: SDD) is a key variable for assessing environmental changes in lakes. Using remote sensing we calculated and elucidated the SDD dynamics in lakes in the Inner Mongolia-Xinjiang Lake Zone (IMXL) from 1986 to 2018 in response to variations in temperature, rainfall, lake area, normalized difference vegetation index (NDVI) and Palmer's drought severity index (PDSI). The results showed that the lakes with high SDD values are primarily located in the Xinjiang region at longitudes of 75°-93° E. In contrast, the lakes in Inner Mongolia at longitudes of 93°-118° E generally have low SDD values. In total, 205 lakes show significant increasing SDD trends ($P<0.05$), with a mean rate of 0.15 m per decade. In contrast, 75 lakes, most of which are located in Inner Mongolia, exhibited significant decreasing trends with a mean rate of 0.08 m per decade ($P<0.05$). Pooled together, an overall increase is found with a mean rate of 0.14 m per decade. Multiple linear regression reveals that among the five variables selected to explain the variations in SDD, lake area accounts for the highest proportion of variance (25%), while temperature and rainfall account for 12% and 10%, respectively. In addition, rainfall accounts for 52% of the variation in humidity, 8% of the variation in lake area and 7% of the variation in NDVI. Temperature accounts for 27% of the variation in NDVI, 39% of the variation in lake area and 22% of the variation in PDSI. Warming and wetting conditions in IMXL thus promote the growth of vegetation and cause melting of glaciers and expansion of lake area, which eventually leads to improved water quality in the lakes in terms of higher SDD. In contrast, lakes facing more severe drought conditions, became more turbid.

Keywords: Inner Mongolia-Xinjiang Plateau; lakes; transparency; climate change

1. Introduction

Lakes are of vital importance because they provide multiple socioeconomic and ecosystem services, including water for drinking and irrigation and places generating tourism, to the fast growing human populations of the world (Zhang et al. 2017). The water clarity of lakes is generally quantified as the Secchi disk depth (SDD, in meter), which is the depth at which a black-white Secchi disk can no longer be seen when deployed in water. Due to the simplicity and low cost of SDD measurements and their important function in assessing the underwater light climate in lakes and the consequent productivity of planktonic and benthic algae and aquatic macrophytes (Lee et al. 2015), numerous studies conducted over the past five decades have focused on monitoring the changes in SDD of ocean and lake ecosystems (Binding et al. 2007; Liu et al. 2020; Olmanson et al. 2008; Shen et al. 2020). The water quality of Lake Hongze, Lake Taihu, and Lake Liangzi has been reported to have deteriorated dramatically over the past half-century, with decrease rates of 0.9, 0.5, and 5.0 cm/year (Li et al. 2019; Shi et al. 2018; Xu et al. 2018), respectively. The lakes of northeastern North America and Europe (Williamson et al. 2015), Chesapeake Bay (Lefcheck et al. 2017) and the southern and central North Sea (Capuzzo et al. 2015) have shown similar patterns. Conversely, many studies have reported increasing SDD over time. For example, Feng et al. (2019) reported that many Yangtze lakes in China, showed increasing SDD during 2003−2016. Liu et al. (2020) and Shen et al. (2020) reported that the water SDD of Chinese lakes has increased over the past two decades. In addition, the average SDD of three of America's great lakes, Ontario, Huron, and Michigan increased by 58%, 49% and 62% from 1978 to 2014

(Binding et al. 2015). The SDD time series in the Río Tercero Reservoir of Argentina exhibited an increasing trend from 2003 to 2010 (Bonansea et al. 2015). Similarly in the global ocean, the mean SDD increased at a rate of 0.04 m/year (p=0.05) from 2000-2010 (He et al. 2017). Moreover, most lakes exhibit a gradual rise or fall or no distinct trend (Guan et al. 2011).

The variability in water clarity is in part related to climate conditions (Olmanson et al. 2008; Pekel et al. 2016). As the global mean annual air temperature has increased in recent decades, many large lakes have exhibited symptoms of eutrophication and water quality deterioration (Qin et al. 2019). It remains unclear whether rainfall deteriorates or improves water quality. The inflow caused by rainfall may deliver suspended materials, dissolved solids and nutrients from watersheds to lakes, thereby increasing lake water turbidity (Bonansea et al. 2015). Conversely, the increase in rainfall may greatly promote the dilution of suspended matter, thereby increasing lake clarity (Hou et al. 2017). In addition to air temperature and rainfall, wind may also affect SDD through resuspension of lake sediment and is of importance in shallow lakes (Cao et al. 2017; Hou et al. 2017; Shi et al. 2018).

Human activities have also affected the water quality of the world's lakes. Among the eastern lakes of China, water clarity has been particularly susceptible to changes in chemical fertilizer use and wastewater discharge (Feng et al. 2019). However, other drivers can also be important, such as severe sand dredging and gold-mining activities (Cao et al. 2017; Lobo et al. 2015) as well as shifts in the hydrological regime resulting from dam construction in associated lakes such as Lake Poyang and Lake Dongting (Feng et al. 2013). Research shows that the type of land cover surrounding a lake is closely

related to the lake and nearshore water quality and that the surrounding vegetation plays a notable role in reducing soil erosion and purifying inflow water (Olmanson et al. 2014). Urban surroundings produce more stormwater runoff and therefore much higher levels of nitrogen and phosphorus than other land surfaces (Tong and Chen 2002).

Most long-term studies of SDD and the drivers behind changes over time have been restricted to a relatively small number of lakes or special regions. The SDD responses to climate and human activities, however, vary among lakes and climate regions, and there is a need to investigate the long-term trend of lake SDD in arid-semiarid climate regions and to clarify the driving mechanisms of SDD variations.

The lakes in the Inner Mongolia-Xinjiang Lake Zone (IMXL) are internal drainage systems in an arid or semiarid climate and they are sensitive and vulnerable to climate change (Tao et al. 2015). Studies by Tao et al. (2015) and Zhang et al. (2019) provided a comprehensive satellite-based evaluation of lake surface changes across the IMXL between the late 1980s and 2010. However, an effective assessment of water resources should focus not only on water quantity but also on water quality. Long-term trends in the water quality of lakes are often early warning indicators of significant local, regional or global changes (O'Reilly et al. 2015). Understanding water quality patterns, trends and drivers is necessary for designing effective management and remediation strategies. Unfortunately, research into the water clarity in this region has not yet been undertaken. Recently, the cloud-based parallel-computing platform of Google Earth Engine (GEE) has made it possible for researchers to leverage high-resolution, freely accessible satellite imagery over large areas (Pekel et al. 2016), thereby enabling research on deforestation, drought, disaster, disease, food security, water management, climate monitoring and

environmental protection at a global scale (Gorelick et al. 2017). Thus, in this study, we used the GEE platform to conduct a case study of the IMXL to thoroughly examine the annual lake (> 0.1 km^2) SDD dynamics from 1986 to 2018 in the area. In addition, we quantified the relative contributions of climate warming and wetting to SDD variations in the IMXL (Fig. S1, Process 3).

2. Materials and Methods

2.1 Study area

The Inner Mongolia-Xinjiang Plateau is located at the middle latitudes in the hinterland of Eurasia. It covers an area of approximately 3.75 million km^2 and has an average elevation of 1,546 m and a population of approximately 144 million (National Bureau of Statistics of China 2017). In the region, covering more than 4,000 km from east to west, the environmental and vegetation conditions are highly diverse (Li et al. 2012). For example, the annual precipitation ranges from 25 mm to 400 mm and the moisture conditions vary from semihumid to semiarid to arid. The vegetation types also shift accordingly – from meadow to typical and desert steppes, to the Gobi Desert and typical deserts (Li et al. 2012). There are nearly 750 IMXL lakes (> 0.1 km^2) distributed across the area with a cumulative water surface area of approximately 16,800 km^2 (Zhang et al. 2019). Most of the lakes on the Inner Mongolia-Xinjiang Plateau are surrounded by vast grasslands, which have nourished the Mongolian people and created a unique Mongolian nomadic civilization. Many of the lakes on the plateau are internationally important wetlands for threatened animal species and migratory waterfowl (Tao et al.

2015). In recent decades, increasing rainfall and air temperature have created a warming and wetting environment on part of the plateau (Fig. 1), which offers favor conditions for vegetation (Piao et al. 2006).

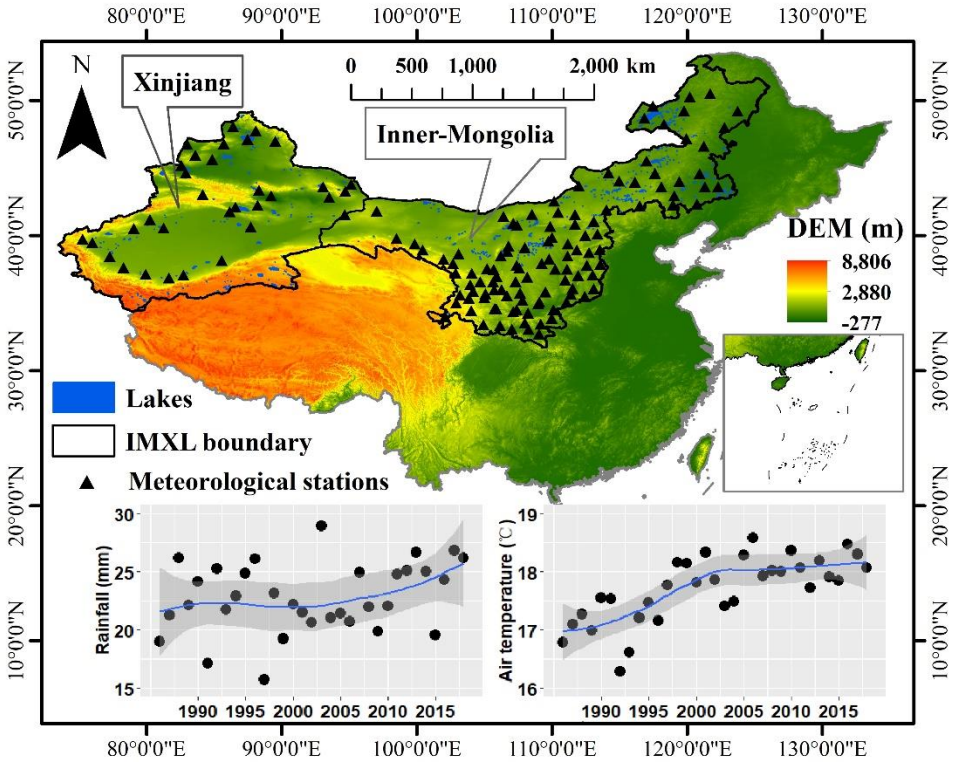

Fig. 1. Digital elevation model (DEM) of the continent, distribution of the IMXL lakes and meteorological stations and long-term climate (rainfall and air temperature) trends in the IMXL region. The IMXL region can be administratively divided into Xinjiang and Inner-Mongolia.

2.2 Lake boundary and area definitions

The global water occupancy frequency dataset (Pekel et al. 2016) was used to identify lake surfaces. This dataset was generated using more than 3,865,000 scenes from the Landsat TM, ETM+ and OLI with information on water occurrence frequency from 1984 to 2015. We retained the original frequency values and assumed occurrence frequencies of ≥25%, ≥50%, ≥75% and ≥100% to identify permanent water surfaces. Water surfaces were then trimmed from enlarged IMXL lake boundaries with a 2 km buffer to obtain permanent IMXL lake surfaces (Fig. S1, Process 1). Friedl and Sulla-Menashe (2019) and Sophie et al. (2010) mapped global water surfaces at spatial resolutions of 500 and 300 m, respectively. By comparing the performance of the estimated lake surface area results at these four thresholds and from previous studies, we selected the most suitable approach to define the permanent water bodies of the IMXL. The yearly water surface areas of IMXL lakes were therefore derived from the selected approach (Supplementary Text 1).

2.3 Satellite data and SDD estimation model

Lake water SDD was calculated from 49150 images (15.6 trillion bytes) of Landsat TM, ETM+ and OLI data for the study area from June to October between 1986 and 2018 (Fig. S2), obtained from the United States Geological Survey. The Landsat Collection 1 Tier 1 images were subjected to geometric and atmospheric corrections as well as cross-calibration among the different sensors (Wulder et al. 2016). For each image, clouds, cloud shadows and snow pixels were removed by using the data quality layer from the cloud masking method called “CFmask”, which is effective and suitable for preparing Landsat data for change detection (Zhu and Woodcock 2014). Terrain shadows were

identified and removed by using the solar azimuth and zenith angles from Landsat images and the digital elevation model (DEM) from the Shuttle Radar Topography Mission (Zhu and Woodcock 2014). All the remaining pixels were considered good-quality observations that could be used for open surface water SDD mapping. Finally, annual cloud- and snow-free image collections comprising all Landsat TM, ETM+ and OLI images in the study area were generated based on the GEE cloud-based parallel-computing platform.

In a previous study, Zhang et al. (2021) calibrated and validated an empirical SDD algorithm based on hundreds of in situ SDD measurements and concurrent Landsat images for lakes in China (Fig. S1, Process 2 and Fig. S3). The algorithm provides a reliable estimate of the SDD with a mean relative error and a normalized root mean square error of 34.2% and 55.4%, respectively. The algorithm was therefore used to estimate the SDD of the IMXL in this study, and spatial-temporal SDD characteristics of lakes with water areas $\geq$0.1 km^2 were produced from qualified cloud-free Landsat series images in the nonfreezing period from June to October between 1986 and 2018.

2.4 Meteorological, normalized difference vegetation index (NDVI) and Palmer's drought severity index (PDSI) datasets

Data on the monthly rainfall and temperature from June to October between 1986 and 2018 were downloaded from China Meteorological Administration stations (http://data.cma.cn). A total of 146 observation stations are distributed across the IMXL (Fig. 1). Precipitation scours the drainage area (Bonansea et al. 2015), and temperature

influences the growth of the surrounding vegetation (Liu et al. 2016); therefore, these two natural factors were included to examine their impacts on the interannual changes in water SDD.

NDVI is a measure of vegetation growth in the drainage basin of a lake through the impact of soil erosion conditions. NDVI is widely used for long-term monitoring of vegetation biomass (Gamon et al. 2013). The annual NDVI dataset used in this research (https://www.ncdc.noaa.gov/) covers the period 1986-2018, with a spatial resolution of 0.05° (Vermote et al. 2014). The annual NDVI data were used to examine the influence of the drainage erosion status on the interannual SDD variations.

For an index of the balance between evaporation and precipitation, we used average monthly estimates of PDSI provided by Abatzoglou et al. (2018) from the National Climate Data Center (https://www.ncdc.noaa.gov/) to calculate their contribution to water SDD variations. PDSI values lower than -0.5 indicate drought conditions, values between -0.5 and 0.5 indicate near-normal conditions, and values larger than 0.5 indicate humid conditions (Yan et al. 2016). PDSI has previously been proven to be an effective indicator of long-term climate effects on lake water clarity (Leach et al. 2019). We used the annual PDSI dataset with a period of 1986-2018 and a spatial resolution of 0.01° to examine the impact of PDSI on the interannual changes in the water SDD.

2.5 Trend and correlation analysis

The annual mean SDD and driving factors from 1986 to 2018 were calculated for the entire IMXL and for each lake. We assumed that the rate of change in SDD in the

short term was linear with a constant coefficient. Thus, SDD in a year without images could be obtained by interpolating the data before and after this particular year. Linear regression was performed among the 38 annual values to obtain the rate of change in water SDD and the driving factors during the study period. The mean SDD values of seven subperiods (1986-1990, 1991-1995, 1996-2000, 2001-2005, 2006-2010, 2011-2015 and 2016-2018) and the entire study period were calculated.

The in situ rain and air temperature data were first interpolated with the inverse distance weighting method and then extracted within each lake region. Raster PDSI and NDVI data were extracted within a 20 km ring buffer outside the lake boundary. We performed a correlation analysis to identify the direction (negative or positive) and strength of the relationship between lake SDD and the mean value of each extracted variable. The P-values associated with the correlation analysis for each variable were also obtained, and a P-value of <0.05 indicates that the contribution of the variable is statistically significant. We defined the importance as the proportionate contribution of each explanatory variable makes to the determination coefficient by using a multiple linear analysis method (Asoka et al. 2018) in RStudio software with R version 3.5.0. The increase in the determination coefficient when including the new variable was ascribed to the absolute contribution of the explanatory variable to the SDD, lake area, NDVI and PDSI variations.

3. Results

3.1 Long-term trends of five explanatory variables

The rainfall in the entire study region showed an increasing trend, with a mean increasing rate of 0.76±0.23 mm/year (Fig. 1). However, major regional differences occurred. The rainfall in Xinjiang and the western region of Inner Mongolia showed a significant increasing trend, while a significant decreasing trend was found in the eastern region of Inner Mongolia (Fig. 2a). The temperature of the entire IMXL area (except for the black-colored region in Fig. 2b) showed a significant increasing trend, although, with a mean rate of increase of 0.04±0.14 ℃/year (Fig. 2b). By contrast, the PDSI of the entire study region showed a decreasing trend with mean rate of -0.04±0.07/year. However, in most regions of the IMXL the trends were statistically insignificant (Fig. 2c). The NDVI of the entire study region showed an increasing trend, with a mean rate of 0.04±0.11%/year, while the trends in most regions of IMXL were not significant (Fig. 2d). The lake area of the entire study region showed an increasing trend, with a total rate of 12.17 km^2/year and a mean rate of 0.074±1.88 km^2/year; 92% of lakes in the regions of Xinjiang exhibited a significant increasing trend, and the lakes with a decreasing trend in the study area were almost all located in Inner-Mongolia (Fig. 2e).

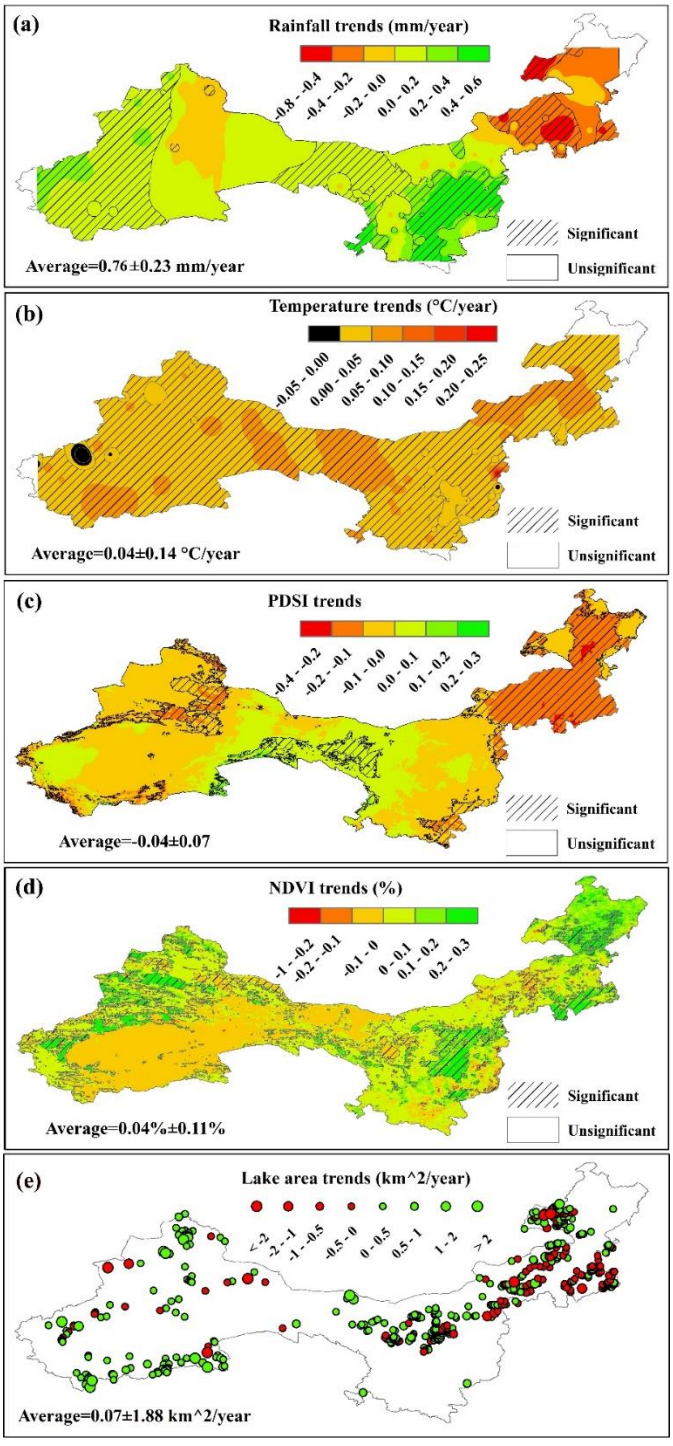

Fig. 2. Long-term trends of rainfall (a), temperature (b), PDSI (c), NDVI (d) and lake area (e) from 1986 to 2018; the critical values at which the relationships are statistically

significant for the positive or negative correlation coefficients ($p<0.05$) are filled in with diagonal stripes in (a)-(d).

3.2 Lake surface extraction

Effective definition of lake boundaries is a critical step for the long-term derivation and comparison of lake SDD. For this purpose, the performance of lake surface extraction at thresholds of ≥25%, ≥50%, ≥75% and ≥100% as well as findings from previous studies by Friedl and Sulla-Menashe (2019) and Sophie et al. (2010) were compared, as shown in Fig. S4 and Fig. S5. The histograms of the lake surface area were more evenly distributed at thresholds of ≥25%, ≥50% and 75% and from Sophie et al. (2010) compared with those at a threshold of ≥100% and from Friedl and Sulla-Menashe (2019). The lake surface results at thresholds of ≥25% and ≥50% included seasonal and transient water bodies, while the results at a threshold of ≥100% and from Friedl and Sulla-Menashe (2019) eliminated most year-long water pixels, resulting in a false conclusion whereby no large lakes were detected (Fig. S4). Lake surface determination using the global land cover dataset (300×300 m) from Sophie et al. (2010) achieved a better performance in detecting large lakes, and this result also included seasonal and transient water bodies, which should be eliminated from year-long water body detection (Fig. S4f). In contrast, the result at thresholds of ≥75% not only retained the complete information of all lakes but also removed the influence of seasonal water body changes. We also compared the longitudinal distributions in lake areas from the six methods. The result at a threshold of ≥25% and from Sophie et al. (2010) overestimated the total lake area in the IXML, while the result at a threshold of ≥100% and from Friedl and Sulla-Menashe (2019)

underestimated the lake area (Fig. S5). Therefore, we used a threshold of ≥75% to define the year-long water bodies of the IMXL lakes.

3.3 Spatial distribution of the IMXL lakes SDD

Quality-controlled Landsat 5 TM, 7 ETM+ and 8 OLI R_{rs} data between 1986 and 2018 were used to generate annual SDD maps within the lake boundaries and mean values between 1986 and 2018 for the entire IMXL were estimated, as shown in Fig. 3. The SDD value of all IMXL lakes was estimated to be 0.92±0.87 m. The lakes with high SDD values are primarily located in the Xinjiang region with longitudes of 75°-93° E, and few high-SDD lakes are located in Inner Mongolia with longitudes of 118°-122° E. In contrast, the lakes in Inner Mongolia with longitudes of 93°-118° E generally have low SDD values (Fig. 3). The clearest lake is the typical deep saltwater lake of Sayram (44.60° N, 81.17° E) with a mean estimated SDD value of 3.15 m, which is very close to the value documented by Huo et al. (2015).

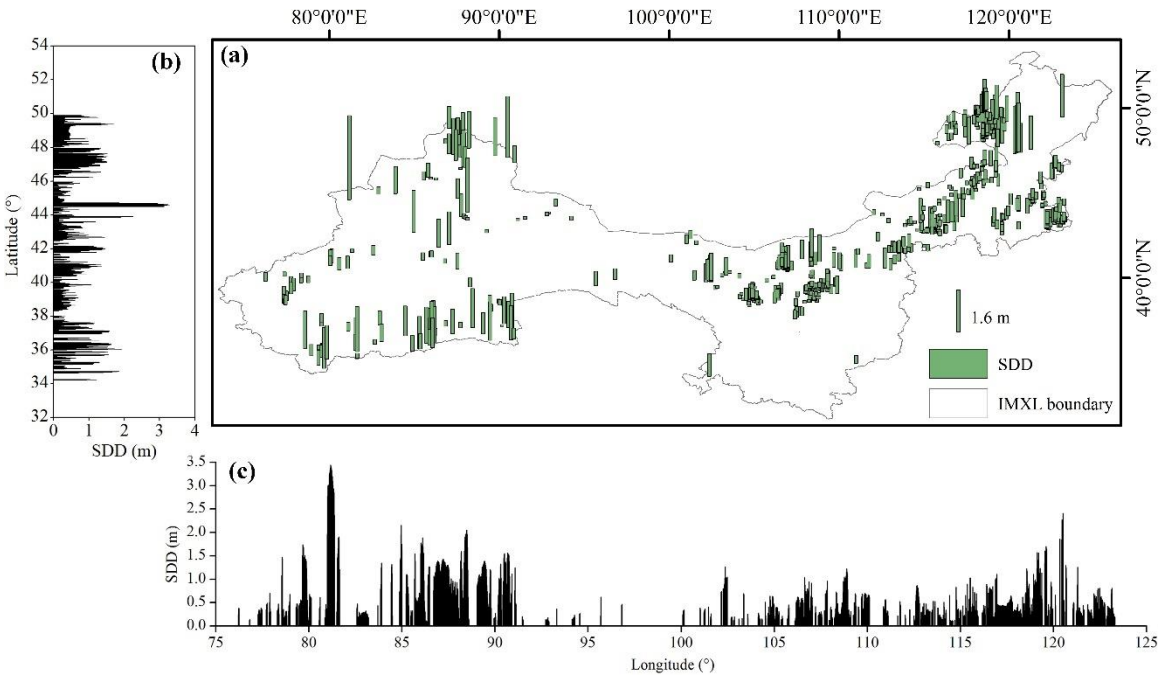

Fig. 3. Spatial distributions of the IMXL SDD (a) and SDD variation versus latitude (b) and longitude (c) at a spatial resolution of 0.01° × 0.01°. Each SDD pixel was averaged from 1986 to 2018.

3.4 Temporal distributions of the IMXL lakes SDD

The number of lakes distributed per SDD level (<0.5, 0.5-1, 1-1.5, 1.5-2 and ≥2 m) among the seven periods (1986-1990, 1991-1995, 1996-2000, 2001-2005, 2006-2010, 2011-2015, and 2016-2018) and a transition map between each period and the next are presented in Fig. 4 to display the change patterns of the different SDD levels. Of the 594 lakes, >64% had SDD values lower than 0.5 m in the seven periods. For lakes with lower SDD levels (<0.5 and 0.5-1), a total of 262 lakes underwent a transition to a clearer SDD level, and 133 lakes changed to more turbid conditions. In contrast, for lakes with higher SDD levels (1.5-2 and ≥2 m), a total of 11 lakes experienced a transition to a clearer SDD

level, and 39 lakes displayed more turbid conditions. Generally, a total of 307 lakes had transitions to clearer SDD levels and 236 lakes to more turbid conditions in the six transitions, suggesting that the SDD of lakes in the IMXL generally increased over the past 33 years.

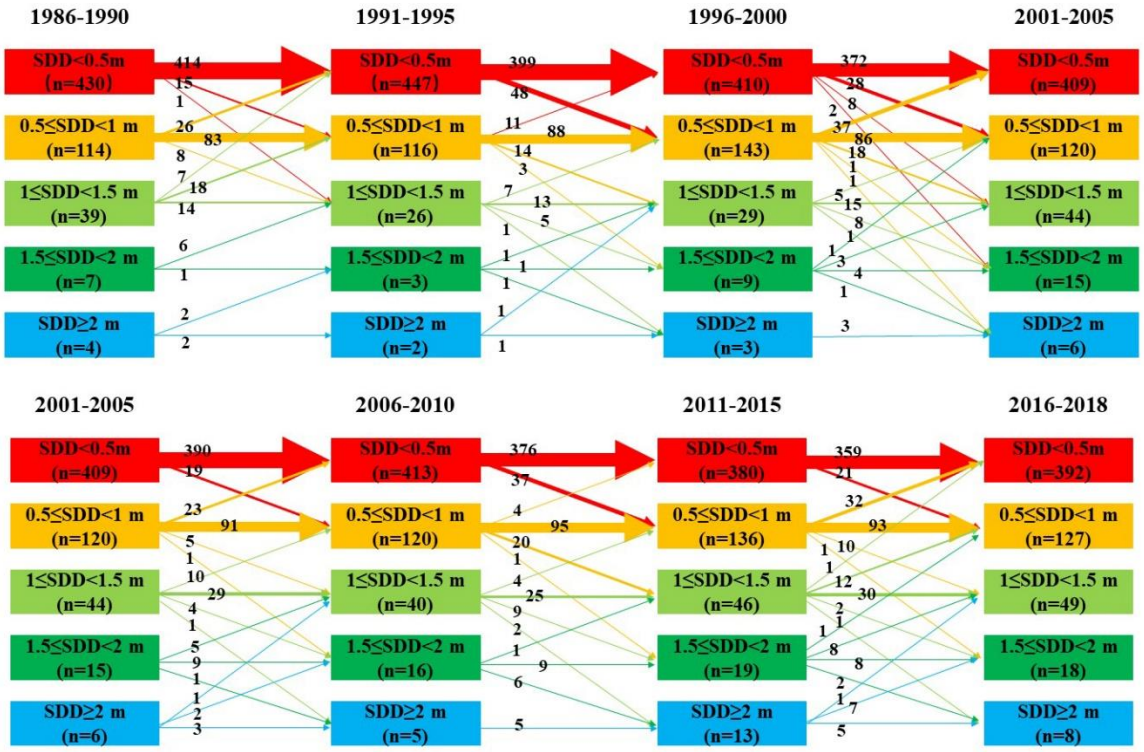

Fig. 4. Number of lakes with different SDD levels (<0.5, 0.5-1, 1-1.5, 1.5-2 and ≥2 m) that showed a transition to other SDD levels from each period to the next. The widths of the arrow indicate the number of changed lakes.

The yearly trends in the IMXL from 1986-2018 revealed both increasing and decreasing trends. Statistically, 355 lakes exhibited increasing trends, while 205 lakes exhibited decreasing trends. Of all the lakes, 205, mostly located in Xinjiang and the western part of Inner Mongolia, showed significant increasing trends. There were 75

lakes, mainly located in the eastern part of Inner Mongolia, that exhibited significant decreasing trends (Fig. 5a). The normalized SDD of 205 lakes displayed a significant increasing trend of 0.26 (equivalent to a rate of increase of 0.15 m) per decade (Fig. 5b), while the normalized SDD of 75 lakes with a significant decreasing trend had an average rate of 0.22 (0.08 m per decade) (Fig. 5c). The average SDD of the 594 IMXL lakes showed significant increasing trends from 1986-2018, with a rate of change of 0.14 m per decade (Fig. 5d).

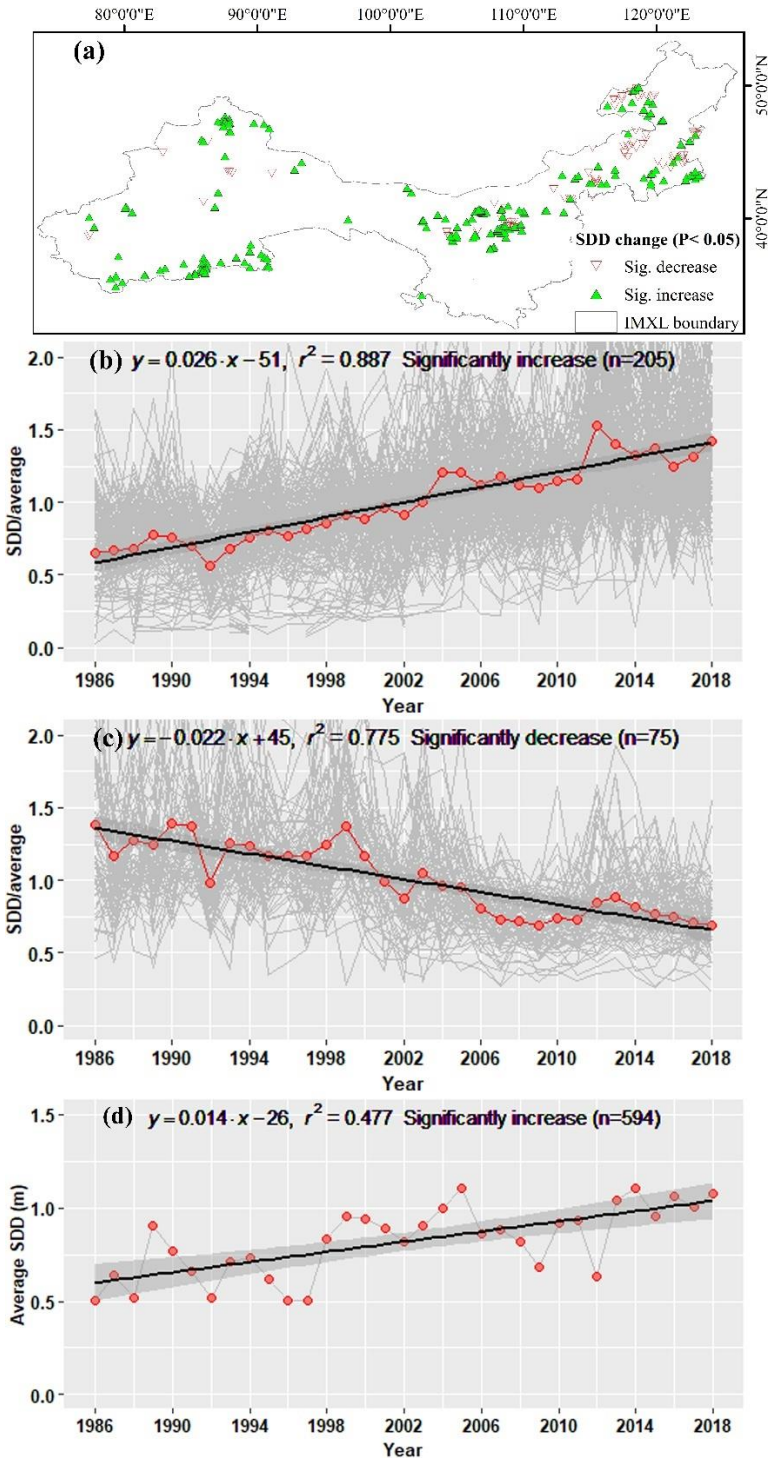

Fig. 5. Spatial distribution of IMXL lakes with significant changes in water SDD from 1986 to 2018 (a). A total of 205 lakes showed significant increasing trends (b), and 75 lakes exhibited significant decreasing trends (c). The average SDD of 594 lakes displayed

a significant increasing trend (d). The red points were averaged from all lakes demonstrating a significant increase or decrease.

4. Discussion

4.1 Correspondence among the long-term trends

To better understand the influence of various factors on the water SDD for IMXL lakes, we examined the correlations between the annual SDD and the potential driving factors for all and each of the 594 lakes. For all five factors analyzed (rainfall, temperature, PDSI, NDVI and lake area), both positive and negative correlations were observed (Figs. 6, S6). At the regional level, a significant positive correlation was observed between the long-term mean SDD and rainfall ($r=0.54$; $P<0.05$) (Fig. S6a). Specifically, the annual SDD demonstrated significant positive correlations with rainfall for 87 lakes, suggesting that lake SDD increased with increasing rainfall and that rain diluted the turbid water in this area. However, there was an inconsistency for 5 lakes showing significant negative correlations between SDD and rainfall (Fig. 6g). These correlations could be possibly attributed to rainfall leaching, which played a role in regulating lake SDD in these lakes by delivering suspended materials, dissolved solids and nutrients from watersheds to lakes (Bonansea et al. 2015; Pi et al. 2020). Land cover changes in the IMXL region may indirectly affect SDD by impacting nutrient and particulate matter loading. At the regional level, a significant positive correlation was observed between the long-term mean SDD and NDVI ($r=0.52$; $P<0.05$) (Fig. S6d). Specifically, the annual mean SDD showed significant positive correlations with NDVI

for 76 lakes and with PDSI for 108 lakes, suggesting that the humid environment boosts vegetation growth and nutrient uptake, leading to an increasing SDD. Although the increasing rainfall in the basins of IMXL lakes might trigger sediment inflow from upstream areas, it appears that filtration through the surrounding vegetation counteracts these effects for these lakes. This is consistent with the findings of Wang et al. (2016), showing that increasing vegetation in the Yellow River Basin rapidly reduced soil erosion. At the regional level, significant positive correlations were observed between the long-term mean SDD and lake area ($r=0.56$; $P< 0.05$) (Fig. S6e) and between the long-term mean SDD and temperature ($r=0.65$; $P<0.05$) (Fig. S6b). Specifically, the annual SDD was significantly positively correlated with lake area for 241 lakes and with temperature for 94 lakes, indicating that both lake expansion and warming contributed to the increasing SDD in these regions. However, there was an inconsistency for 43 lakes, showing significant negative correlations between SDD and temperature (Fig. 6g). These correlations could be possibly attributed to the increasing chlorophyll-a induced by climate warming (Liu et al. 2019), which overwhelmed the effects of lake expansion for most lakes and resulted in a negative correlation between the SDD and lake area (Fig. 6j).

Spatially, the IMXL lakes could be divided into four groups (I, II, III and IV), as shown in Fig. 6a. In Groups I and III, the annual mean SDD of most lakes showed significant positive correlations with rainfall and NDVI, suggesting that greening vegetation and dilution resulting from increasing rainfall were the primary triggers of the increasing SDD. For most of the lakes in Group II, rainfall, lake SDD and lake area all showed significant decreasing trends. The strong relationship of lake SDD with rainfall and lake area indicated that lake shrinkage was the main cause of water deterioration. A

few lakes became clearer as a result of lake expansion and increasing NDVI. The increasing lake clarity and strong linear relationships between lake SDD and lake area as well as temperature in the lakes in Group IV (Fig. 6 and Fig. S7) indicated that lake expansion was the reason for the improved clarity of the lakes in Group IV, possibly reflecting melting of glaciers due to the rising temperature in the region.

Multiple linear analysis (Fig. 7) revealed that the five variables (NDVI, PDSI, rainfall, temperature and lake area) explained 68% of the SDD variation, with lake area contributing the most (0-83%, mean 25%) to the variations, while the mean contributions of PDSI, rainfall and NDVI were 10% and that of temperature was 12% (Fig. 7a). Rainfall and temperature explained 47% of the lake area variation, with temperature contributing the most (mean 39%) and rainfall the least (mean 8%) (Fig. 7b). Together, PDSI, rainfall and temperature explained 42% of the NDVI variation, and temperature contributed the most (mean 27%), followed by PDSI (mean 8%) and rainfall (mean 7%) (Fig. 7c). Rainfall and temperature explained 73% of the PDSI variation; the mean contribution of rainfall was 52%, and that of temperature was 22% (Fig. 7d). On the basis of our observations, we drew a mechanism diagram of the long-term variations in SDD and related environmental factors (Fig. 7e-f). In general, the warming and wetting conditions in the IMXL promote vegetation growth, enhance glacier melting and expand the lake area, finally inducing improved lake water quality. In contrast, lakes facing more severe drought conditions (mostly situated in the eastern part of Inner Mongolia) became more turbid.

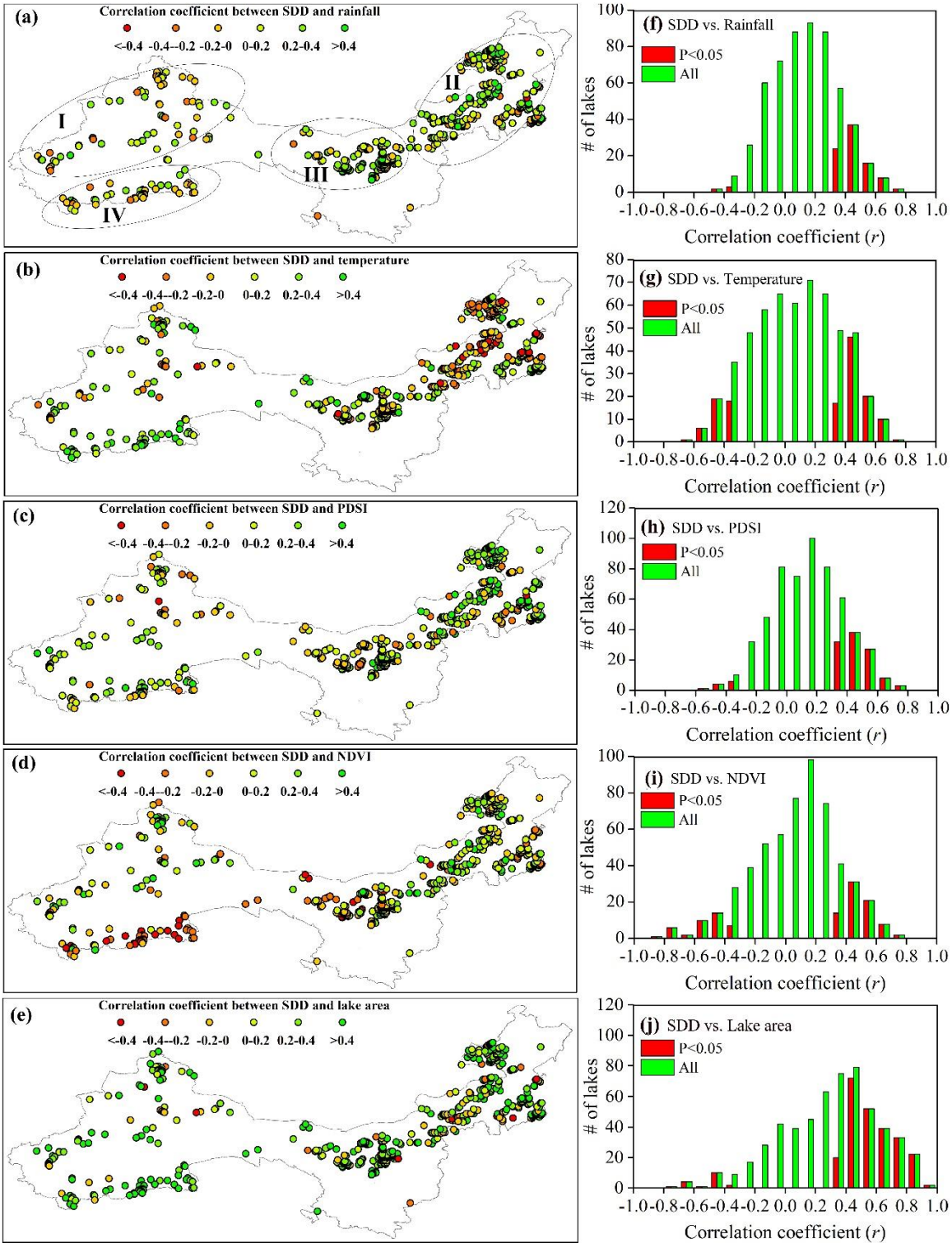

Fig. 6. Correlation coefficients between long-term SDD and the four explanatory variables for each IMXL lake from 1986 to 2018. (a) Correlation coefficient between

long-term SDD and rainfall, (b) correlation coefficient between long-term SDD and temperature, (c) correlation coefficient between long-term SDD and PDSI, (d) correlation coefficient between long-term SDD and NDVI, and (e) correlation coefficient between the long-term SDD and lake area. The IMXL lakes were divided into four groups (I, II, III and IV). In Groups I and III, SDD increased in most lakes due to greening vegetation and lake expansion from increasing rainfall. Most deteriorating lakes belonged to Group II, and the decreasing trend reflected lake shrinkage due to long-term drought. A few lakes became clearer as a result of increasing NDVI. In Group IV, the SDD increased in response to lake expansion resulting from melting glaciers as a consequence of the rising temperature. Histograms are shown of the correlation coefficients between yearly SDD and rainfall (f), air temperature (g), PDSI (h), NDVI (i) and lake area (j) for each lake. Red indicates the critical values at which the relationships are statistically significant for the positive or negative correlation coefficients (e.g., $P< 0.05$).

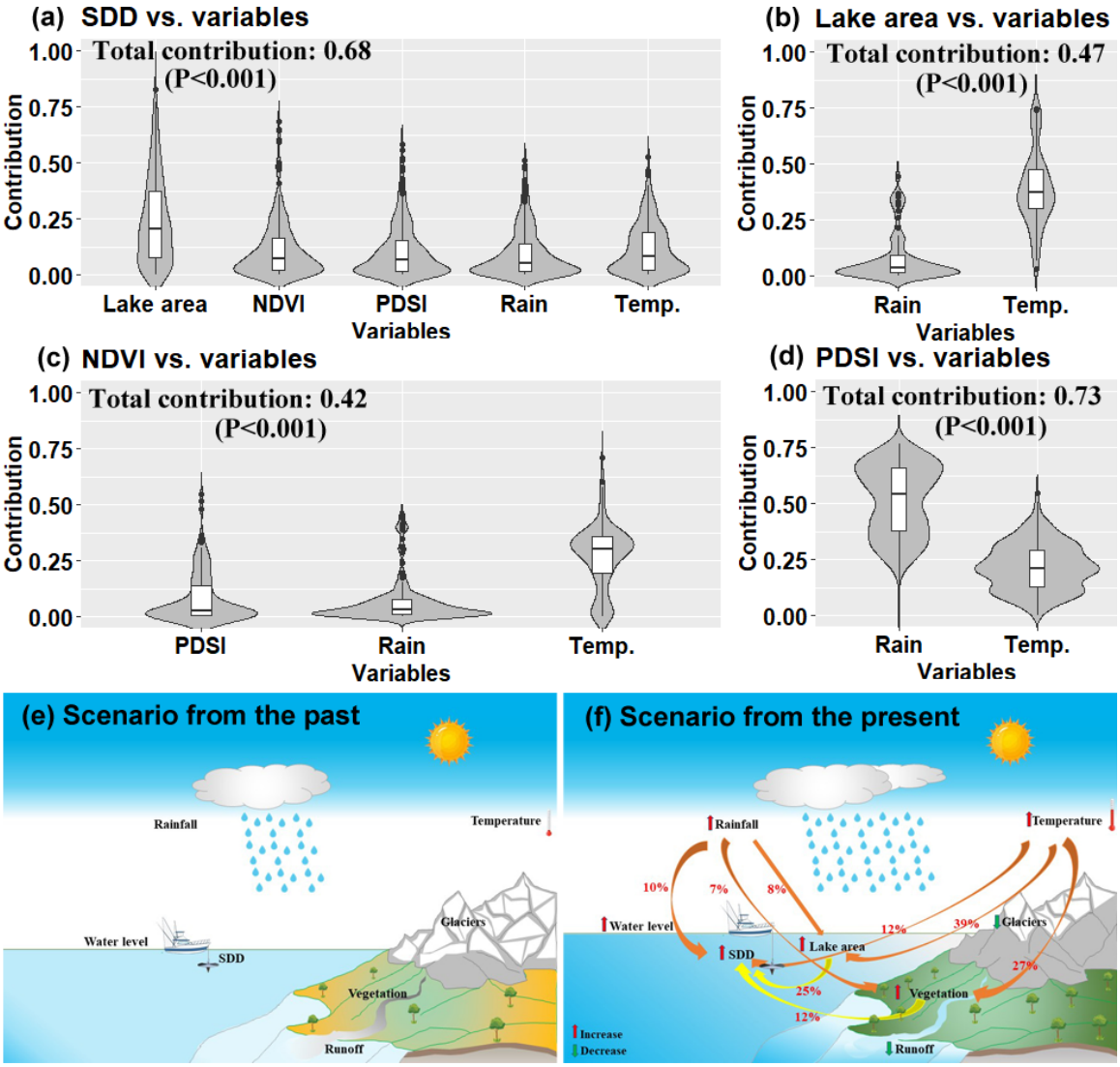

Fig. 7. The contributions of the explanatory variables to SDD, NDVI, lake area and PDSI variations for each affected IMXL lake. Violin and box plots of the absolute contributions of the five variables (lake area, NDVI, PDSI, rainfall and temperature) to the SDD variation; the five variables explain 68% of the SDD variation (a). Violin and box plots of the absolute contributions of the two variables rainfall and temperature to the lake area variation; the two variables explain 47% of the lake area variation (b). Violin and box plots of the absolute contributions of the three variables PDSI, rainfall and temperature to

the NDVI variation; the three variables explain 42% of the NDVI variation (c). Violin and box plots of the absolute contributions of the two variables rainfall and temperature to the PDSI variation; the two variables explain 73% of the PDSI variation (d). Scenarios from the past (e) and the present (f) and absolute contributions of all explanatory variables to the SDD, NDVI and lake area variations.

4.2 Implications and management of water quality for lakes in the IXML

Due to the remote distance, low temperature and extreme environment of the IMXL, the traditional ship-based observation method is insufficient at certain temporal and spatial scales. By using long-term satellite observations, a systematic investigation and exploration of the spatiotemporal variations and long-term trend of SDD in response to variations in temperature, rainfall, lake area, NDVI and PDSI was conducted in the IMXL, which served as a solid basis for use in future water monitoring and management in this arid-semiarid climate region.

Our study suggests that the SDD variations were associated with lake expansion, temperature, precipitation and vegetation, which were closely linked to climate change. The warming conditions in the IMXL over the past few decades have been proven to enhance glacier melting and expand the lake area. The simulated warming trend of the future climate (Barnes et al. 2019) showed that the aquatic environment of the IMXL is expected to experience a substantial change for a certain period. In addition, improved vegetation coverage in catchments has been reported to have positive effects on increasing lake SDD (Liu et al. 2020; Wang et al. 2016). Therefore, more attention must

be paid to climate change and vegetation recovery to design applicable water management plans in the future.

The enhanced SDD may be either detrimental to or beneficial for the aquatic environment. For example, enhanced water clarity has beneficial effects by improving underwater light conditions and promoting submerged vegetation growth and the associated ecology (Zhang et al. 2017). In contrast, enhanced water clarity allows more ultraviolet radiation (UVR) to reach deeper waters, which may substantially inhibit the growth or survival of phytoplankton, zooplankton and fish (Williamson et al. 2001), not least in high-elevation areas. Recent modeling and prediction efforts indicate that ozone depletion will continue well into the new century, and ozone depletion and increased emissions of greenhouse gases (carbon dioxide, methane and nitrous oxide) due to human activities will accelerate global warming (Barnes et al. 2019). In the aquatic habitats of the high-elevation IMXL lakes, increasing water clarity and UVR enhance the possibility that the aquatic environment will be exposed to high levels of UVR, which is potentially damaging to the organisms occupying underwater habitats (Williamson et al. 2001). Within inland lakes, chromophoric dissolved organic matter (CDOM) absorbs a large proportion of light in the ultraviolet spectrum , thereby protecting organisms in the upper euphotic zone from harmful UVR (Aulló-Maestro et al. 2017). Previous studies reported that the concentration of CDOM in IMXL lakes is relatively low in a global context due to limited nutrient inputs from fluvial and other allochthonous land sources (Song et al. 2019; Zhou et al. 2017), which may result in strong photobleaching in an intensive UVR environment and may have negative effects on zooplankton and fish (Williamson et al. 2001).

In summary, the spatiotemporal variations and long-term trends of SDD as well as their responses to climate change revealed in this research have significant implications for water quality monitoring and management for lakes in the IMXL. A comprehensive understanding of climatic impacts on the aquatic ecosystem of the Inner Mongolia-Xinjiang Plateau will require further studies blending long-term reconstructions of observationally constrained water quality with multisource remote sensing data, along with interpretation of climatic factors such as temperature, precipitation, as well as wind, radiation and UVR.

5. Conclusions

The IMXL exhibited both increasing and decreasing trends in water clarity. The lakes, located in the western part of Inner Mongolia, showed significant increasing trends, suggesting that greening vegetation and dilution resulting from increasing rainfall were the primary triggers of the increasing SDD. Some lakes near the border between Xinjiang and Tibet showed significant increasing trends as a result of melting glaciers due to the rising temperature. The lakes in eastern part of Inner Mongolia exhibited significant decreasing trends as a result of lake shrinkage due to severe drought conditions. In general, the warming and wetting conditions in the IMXL promoted the growth of vegetation, caused melting of glaciers and expansion of lake area, and finally improved the water quality of lakes. This study highlights the importance of satellite observations in obtaining large-scale water quality information, and the SDD results from this study provide critical baseline datasets for use in future water quality monitoring efforts.

Author Contributions

Yibo Zhang: Conceptualization, Methodology, Writing - review and editing, Data curation. Kun Shi: Data curation, Writing - review and editing. Yunlin Zhang: Conceptualization, Methodology, Writing - review and editing. Max Jacobo Moreno-Madriñán: Data curation, Writing - review and editing. Xuan Xu: Data curation, Writing - review and editing. Yongqiang Zhou: Data curation, Writing - review and editing. Boqiang Qin: Data curation, Writing - review and editing. Guangwei Zhu: Data curation, Writing - review and editing. Erik Jeppesen: Writing.

Acknowledgments

This work was supported by the National Natural Science Foundation of China (41790423, 41922005, 42007160 and 41771472), the Youth Innovation Promotion Association (CAS) (2017365), and the Key Research Program of Frontier Sciences, Chinese Academy of Sciences (QYZDB-SSW-DQC016). Erik Jeppesen was supported by WATEC (Centre for Water Technology, Aarhus University) and Tübitak BIDEB 2232 (118C250). We thank Anne Mette Poulsen from Aarhus University for editorial assistance and the United States Geological Survey (USGS) for providing all Landsat data. We would also like to thank Na Li and Xiao Sun for their help with field sample collection.

Conflict of Interest

The authors declare that they have no conflicts of interest.

References

Abatzoglou, J.T., Dobrowski, S.Z., Parks, S.A., Hegewisch, K.C., 2018. TerraClimate, a high-resolution global dataset of monthly climate and climatic water balance from 1958–2015. Sci. Data 5, 170191

Asoka, A., Wada, Y., Fishman, R., Mishra, V., 2018. Strong linkage between precipitation intensity and monsoon season groundwater recharge in India. Geophys. Res. Lett. 45, 5536-5544

Aulló-Maestro, M.E., Hunter, P., Spyrakos, E., Mercatoris, P., Kovács, A.W., Horváth, H., Preston, T., Présing, M., Torres Palenzuela, J., Tyler, A., 2017. Spatio-seasonal variability of chromophoric dissolved organic matter absorption and responses to photobleaching in a large shallow temperate lake. Biogeosciences 14, 1215-1233

Barnes, P.W., Williamson, C.E., Lucas, R.M., Robinson, S.A., Madronich, S., Paul, N.D., Bornman, J.F., Bais, A.F., Sulzberger, B., Wilson, S.R., Andrady, A.L., McKenzie, R.L., Neale, P.J., Austin, A.T., Bernhard, G.H., Solomon, K.R., Neale, R.E., Young, P.J., Norval, M., Rhodes, L.E., Hylander, S., Rose, K.C., Longstreth, J., Aucamp, P.J., Ballaré, C.L., Cory, R.M., Flint, S.D., de Gruijl, F.R., Häder, D.-P., Heikkilä, A.M., Jansen, M.A.K., Pandey, K.K., Robson, T.M., Sinclair, C.A., Wängberg, S.-Å., Worrest, R.C., Yazar, S., Young, A.R., Zepp, R.G., 2019. Ozone depletion, ultraviolet radiation, climate change and prospects for a sustainable future. Nat. Sustain. 2, 569-579

Binding, C.E., Greenberg, T.A., Watson, S.B., Rastin, S., Gould, J., 2015. Long term water clarity changes in North America's Great Lakes from multi-sensor satellite observations. Limnol. Oceanogr. 60, 1976-1995

Binding, C.E., Jerome, J.H., Bukata, R.P., Booty, W.G., 2007. Trends in water clarity of the lower great lakes from remotely sensed aquatic color. J. Great Lakes Res. 33, 828-841

Bonansea, M., Rodriguez, M.C., Pinotti, L., Ferrero, S., 2015. Using multi-temporal Landsat imagery and linear mixed models for assessing water quality parameters in Río Tercero reservoir (Argentina). Remote Sens. Environ. 158, 28-41

Cao, Z.G., Duan, H.T., Feng, L., Ma, R.H., Xue, K., 2017. Climate- and human-induced changes in suspended particulate matter over Lake Hongze on short and long timescales. Remote Sens. Environ. 192, 98-113

Capuzzo, E., Stephens, D., Silva, T., Barry, J., Forster, R.M., 2015. Decrease in water clarity of the southern and central North Sea during the 20th century. Global Change Biol. 21, 2206-2214

Feng, L., Hou, X.J., Zheng, Y., 2019. Monitoring and understanding the water transparency changes of fifty large lakes on the Yangtze Plain based on long-term MODIS observations. Remote Sens. Environ. 221, 675-686

Feng, L., Hu, C.M., Chen, X.L., Zhao, X., 2013. Dramatic inundation changes of China's two largest freshwater lakes linked to the Three Gorges Dam. Environ. Sci. Technol. 47, 9628-9634

Friedl, M., Sulla-Menashe, D., 2019. MCD12Q1 MODIS/Terra+ Aqua land cover type yearly L3 global 500m SIN grid V006 [data set]. NASA EOSDIS Land Processes DAAC, 10

Gamon, J.A., Huemmrich, K.F., Stone, R.S., Tweedie, C.E., 2013. Spatial and temporal variation in primary productivity (NDVI) of coastal Alaskan tundra: Decreased vegetation growth following earlier snowmelt. Remote Sens. Environ. 129, 144-153

Gorelick, N., Hancher, M., Dixon, M., Ilyushchenko, S., Thau, D., Moore, R., 2017. Google Earth Engine: Planetary-scale geospatial analysis for everyone. Remote Sens. Environ. 202, 18-27

Guan, X., Li, J., Booty, W.G., 2011. Monitoring Lake Simcoe water clarity using Landsat-5 TM images. Water Resour. Manag. 25, 2015-2033

He, X.Q., Pan, D.L., Bai, Y., Wang, T.Y., Chen, C.-T.A., Zhu, Q.K., Hao, Z.Z., Gong, F., 2017. Recent changes of global ocean transparency observed by SeaWiFS. Cont. Shelf Res. 143, 159-166

Hou, X.J., Feng, L., Duan, H.T., Chen, X.L., Sun, D.Y., Shi, K., 2017. Fifteen-year monitoring of the turbidity dynamics in large lakes and reservoirs in the middle and lower basin of the Yangtze River, China. Remote Sens. Environ. 190, 107-121

Huo, S., Ma, C., Xi, B., Su, J., He, Z., Li, X., 2015. Establishing water quality reference conditions for nutrients, chlorophyll a and Secchi depth for 7 typical lakes in arid and semiarid ecoregion, China. Environ. Earth Sci. 73, 4739-4748

Leach, T.H., Winslow, L.A., Hayes, N.M., Rose, K.C., 2019. Decoupled trophic responses to long-term recovery from acidification and associated browning in lakes. Global Change Biol. 25, 1779-1792

Lee, Z.P., Shang, S.L., Hu, C.M., Du, K.P., Weidemann, A., Hou, W.L., Lin, J.F., Lin, G., 2015. Secchi disk depth: A new theory and mechanistic model for underwater visibility. Remote Sens. Environ. 169, 139-149

Lefcheck, J.S., Wilcox, D.J., Murphy, R.R., Marion, S.R., Orth, R., 2017. Multiple stressors threaten the imperiled coastal foundation species eelgrass (Zostera marina) in Chesapeake Bay, USA. Global Change Biol. 23, 3474-3483

Li, M.M., Liu, A.T., Zou, C.J., Xu, W.D., Shimizu, H., Wang, K.Y., 2012. An overview of the "Three-North" Shelterbelt project in China. For. Stud. China 14, 70-79

Li, N., Shi, K., Zhang, Y.L., Gong, Z.J., Peng, K., Zhang, Y.B., Zha, Y., 2019. Decline in transparency of Lake Hongze from long-term MODIS observations: Possible causes and potential significance. Remote Sens. 11, 177

Liu, D., Duan, H., Loiselle, S., Hu, C., Zhang, G., Li, J., Yang, H., Thompson, J.R., Cao, Z., Shen, M., Ma, R., Zhang, M., Han, W., 2020. Observations of water transparency in China's lakes from space. Int. J. Appl. Earth Obs. 92, 102187

Liu, Q., Fu, Y.H., Zeng, Z., Huang, M., Li, X., Piao, S., 2016. Temperature, precipitation, and insolation effects on autumn vegetation phenology in temperate China. Global Change Biol. 22, 644-655

Liu, X., Feng, J., Wang, Y., 2019. Chlorophyll a predictability and relative importance of factors governing lake phytoplankton at different timescales. Sci. Total Environ. 648, 472-480

Lobo, F.L., Costa, M.P.F., Novo, E.M.L.M., 2015. Time-series analysis of Landsat-MSS/TM/OLI images over Amazonian waters impacted by gold mining activities. Remote Sens. Environ. 157, 170-184

O'Reilly, C.M., Sharma, S., Gray, D.K., Hampton, S.E., Read, J.S., Rowley, R.J., Schneider, P., Lenters, J.D., McIntyre, P.B., Kraemer, B.M., 2015. Rapid and highly

variable warming of lake surface waters around the globe. Geophys. Res. Lett. 42, 10773-10781

Olmanson, L.G., Bauer, M.E., Brezonik, P.L., 2008. A 20-year Landsat water clarity census of Minnesota's 10,000 lakes. Remote Sens. Environ. 112, 4086-4097

Olmanson, L.G., Brezonik, P.L., Bauer, M.E., 2014. Geospatial and temporal analysis of a 20- year record of Landsat- based water clarity in Minnesota's 10,000 lakes. J. Am. Water Resour. Assoc. 50, 748-761

Pekel, J.-F., Cottam, A., Gorelick, N., Belward, A.S.B., 2016. High-resolution mapping of global surface water and its long-term changes. Nature, 540, 418-422

Pi, X., Feng, L., Li, W., Zhao, D., Kuang, X., Li, J., 2020. Water clarity changes in 64 large alpine lakes on the Tibetan Plateau and the potential responses to lake expansion. ISPRS J. Photogramme. 170, 192-204

Piao, S.L., Fang, J.Y., Zhou, L.M., Ciais, P., Zhu, B., 2006. Variations in satellite-derived phenology in China's temperate vegetation. Global Change Biol. 12, 672-685

National Bureau of Statistics of China. 2017. China statistical yearbook. Beijing.

Qin, B.Q., Paerl, H.W., Brookes, J.D., Liu, J.G., Jeppesen, E., Zhu, G.W., Zhang, Y.L., Xu, H., Shi, K., Deng, J.M., 2019. Why Lake Taihu continues to be plagued with cyanobacterial blooms through 10 years (2007–2017) efforts. Sci. Bull. 64, 354-356

Shen, M., Duan, H., Cao, Z., Xue, K., Qi, T., Ma, J., Liu, D., Song, K., Huang, C., Song, X., 2020. Sentinel-3 OLCI observations of water clarity in large lakes in eastern China: Implications for SDG 6.3.2 evaluation. Remote Sens. Environ. 247, 111950

Shi, K., Zhang, Y.L., Zhu, G.W., Qin, B.Q., Pan, D.L., 2018. Deteriorating water clarity in shallow waters: Evidence from long term MODIS and in-situ observations. Int. J. Appl. Earth Obs. 68, 287-297

Song, K.S., Shang, Y.X., Wen, Z.D., Jacinthe, P.-A., Liu, G., Lyu, L.L., Fang, C., 2019. Characterization of CDOM in saline and freshwater lakes across China using spectroscopic analysis. Water Res. 150, 403-417

Sophie, B., Pierre, D., Eric, V., 2010. GlobCOVER 2009 products description and validation report. European Space Agency (ESA) and UCLouvain

Tao, S.L., Fang, J.Y., Zhao, X., Zhao, S.Q., Shen, H.H., Hu, H.F., Tang, Z.Y., Wang, Z.H., Guo, Q.H., 2015. Rapid loss of lakes on the Mongolian Plateau. Proc. Natl. Acad. Sci. U. S. A. 112, 2281-2286

Tong, S.T., Chen, W.L., 2002. Modeling the relationship between land use and surface water quality. J. Environ. Manage. 66, 377-393

Vermote, E., Justice, C., Csiszar, I., Eidenshink, J., Myneni, R., Baret, F., Masuoka, E., Wolfe, R., Claverie, M., 2014. NOAA Climate Data Record (CDR) of normalized Difference Vegetation Index (NDVI), Version 4. NOAA National Climate Data Center

Wang, S., Fu, B., Piao, S., Lü, Y., Ciais, P., Feng, X., Wang, Y., 2016. Reduced sediment transport in the Yellow River due to anthropogenic changes. Nat. Geosci. 9, 38-41

Williamson, C.E., Neale, P.J., Grad, G., De Lange, H.J., Hargreaves, B.R., 2001. Beneficial and detrimental effects of UV on aquatic organisms: Implications of spectral variation. Ecol. Appl. 11, 1843-1857

Williamson, C.E., Overholt, E.P., Pilla, R.M., Leach, T.H., Brentrup, J.A., Knoll, L.B., Mette, E.M., Moeller, R.E., 2015. Ecological consequences of long-term browning in lakes. Sci. Rep. 5, 18666

Wulder, M.A., White, J.C., Loveland, T.R., Woodcock, C.E., Belward, A.S., Cohen, W.B., Fosnight, E.A., Shaw, J., Masek, J.G., Roy, D.P., 2016. The global Landsat archive: Status, consolidation, and direction. Remote Sens. Environ. 185, 271-283

Xu, X., Huang, X.L., Zhang, Y.L., Yu, D., 2018. Long-term changes in water clarity in Lake Liangzi determined by remote sensing. Remote Sens. 10, 1441

Yan, H., Wang, S.Q., Wang, J.B., Lu, H.Q., Guo, A.H., Zhu, Z.C., Myneni, R.B., Shugart, H.H., 2016. Assessing spatiotemporal variation of drought in China and its impact on agriculture during 1982-2011 by using PDSI indices and agriculture drought survey data. J. Geophys. Res. 121, 2283-2298

Zhang, G.Q., Yao, T.D., Chen, W.F., Zheng, G.X., Shum, C.K., Yang, K., Piao, S.L., Sheng, Y.W., Yi, S., Li, J.L., O'Reilly, C.M., Qi, S.H., Shen, S.S.P., Zhang, H.B., Jia, Y.Y., 2019. Regional differences of lake evolution across China during 1960s–2015 and its natural and anthropogenic causes. Remote Sens. Environ. 221, 386-404

Zhang, Y.B., Zhang, Y.L., Shi, K., Zhou, Y.Q., Li, N., 2021. Remote sensing estimation of water clarity for various lakes in China. Water Res. 192, 116844

Zhang, Y.L., Jeppesen, E., Liu, X.H., Qin, B.Q., Shi, K., Zhou, Y.Q., Thomaz, S.M., Deng, J.M., 2017. Global loss of aquatic vegetation in lakes. Earth Sci. Rev. 173, 259-265

Zhou, L., Zhou, Y.Q., Hu, Y., Cai, J., Bai, C.R., Shao, K.Q., Gao, G., Zhang, Y.L., Jeppesen, E., Tang, X.M., 2017. Hydraulic connectivity and evaporation control the water

quality and sources of chromophoric dissolved organic matter in Lake Bosten in arid northwest China. Chemosphere, 188, 608-617

Zhu, Z., Woodcock, C.E., 2014. Automated cloud, cloud shadow, and snow detection in multitemporal Landsat data: An algorithm designed specifically for monitoring land cover change. Remote Sens. Environ. 152, 217-234

Credit Author Statement

Yibo Zhang: Conceptualization, Methodology, Writing - review & editing, Data curation. Kun Shi: Data curation, Writing -review & editing. Yunlin Zhang: Conceptualization, Methodology, Writing - review & editing. Max Jacobo Moreno-Madriñán: Data curation, Writing - review & editing. Xuan Xu: Data curation, Writing - review & editing. Yongqiang Zhou: Data curation, Writing - review & editing. Boqiang Qin: Data curation, Writing - review & editing. Guangwei Zhu: Data curation, Writing - review & editing. Erik Jeppesen: Writing.

Graphical abstract

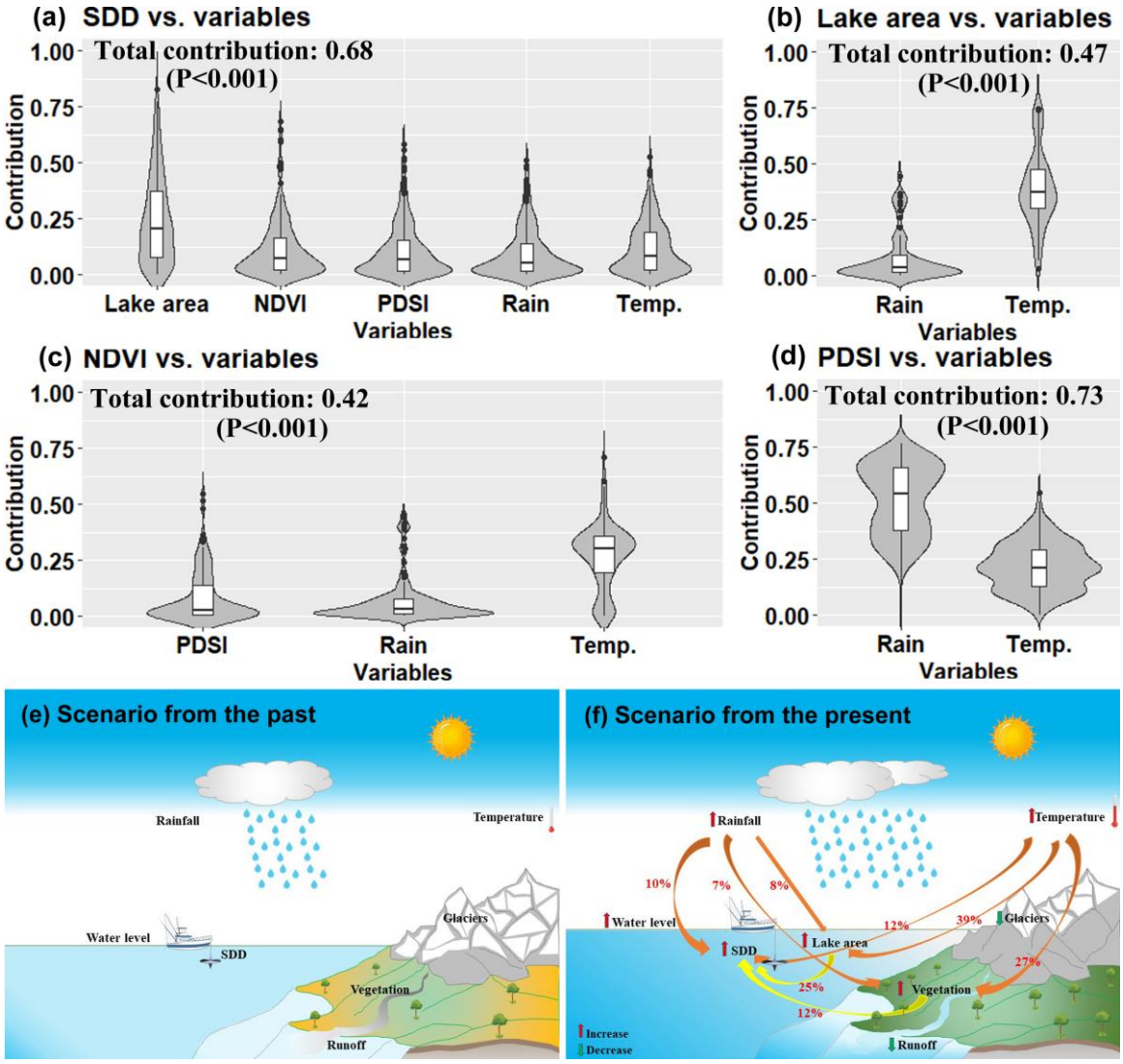

Highlights

The water clarity of 594 year-long lakes in IMXL was documented for the first time;

An overall increasing rate of 0.14 m per decade in water clarity was found in IXML;

Lakes facing more severe drought conditions became more turbid;

Warming and wetting conditions in IMXL improved water quality of the lakes.